Journal of Inorganic Biochemistry 104 (2010) 1164–1170

Contents lists available at ScienceDirect

Journal of Inorganic Biochemistry

journal homepage: www.elsevier.com/locate/jinorgbio

Design of novel iron compounds as potential therapeutic agents against tuberculosis ☆

M. Belén Tarallo [a], Carolina Urquiola [a], Antonio Monge [b], Beatriz Parajón Costa [c], Ronny R. Ribeiro [d], Antonio J. Costa-Filho [d], Roberto C. Mercader [e], Fernando R. Pavan [f], Clarice Q.F. Leite [f], María H. Torre [a,*], Dinorah Gambino [a,*]

[a] Cátedra de Química Inorgánica, Facultad de Química, Universidad de la República, Gral. Flores 2124, C. C. 1157, 11800 Montevideo, Uruguay
[b] CIFA, Universidad de Navarra, Pamplona, Spain
[c] Centro de Química Inorgánica (CEQUINOR/CONICET-UNLP), C.C. 962, Facultad de Ciencias Exactas, Universidad Nacional de La Plata, 1900 La Plata, Argentina
[d] Instituto de Física de São Carlos, Universidade de São Paulo, C.P. 369, 13560, São Carlos, Brazil
[e] Departamento de Física, IFLP-CONICET, Facultad de Ciencias Exactas, Universidad Nacional de La Plata, CC. 67, 1900 La Plata, Argentina
[f] Faculdade de Ciencias Farmacêuticas, Unesp, C.P. 582, 14801-902 Araquara(SP), Brazil

ARTICLE INFO

Article history:
Received 21 May 2010
Received in revised form 1 July 2010
Accepted 9 July 2010
Available online 17 July 2010

Keywords:
Tuberculosis
Iron
Quinoxaline N^1,N^4-dioxides
Mycobacterium tuberculosis

ABSTRACT

In the search for new therapeutic tools against tuberculosis two novel iron complexes, [Fe(L–H)$_3$], with 3-aminoquinoxaline-2-carbonitrile N^1,N^4-dioxide derivatives (L) as ligands, were synthesized, characterized by a combination of techniques, and *in vitro* evaluated. Results were compared with those previously reported for two analogous iron complexes of other ligands of the same family of quinoxaline derivatives. In addition, the complexes were studied by cyclic voltammetry and EPR spectroscopy. Cyclic voltammograms of the iron compounds showed several cathodic processes which were attributed to the reduction of the metal center (Fe(III)/Fe(II)) and the coordinated ligand. EPR signals were characteristic of magnetically isolated high-spin Fe(III) in a rhombic environment and arise from transitions between $m_S = \pm 1/2$ (g_{eff}~9) or $m_S = \pm 3/2$ (g_{eff}~4.3) states. Mössbauer experiments showed hyperfine parameters that are typical of high-spin Fe(III) ions in a not too distorted environment. The novel complexes showed *in vitro* growth inhibitory activity on *Mycobacterium tuberculosis* H_{37}Rv (ATCC 27294), together with very low unspecific cytotoxicity on eukaryotic cells (cultured murine cell line J774). Both complexes showed higher inhibitory effects on *M. tuberculosis* than the "second-line" therapeutic drugs.

1. Introduction

According to WHO (World Health Organization), infectious and parasitic diseases are major causes of human disease worldwide. In particular, tuberculosis (TB), an ancient and currently re-emerging infectious disease, still remains a public health issue at the beginning of the 21st century [1]. This airborne and highly contagious bacterial disease is transmitted from person to person *via* droplets from the throat and lungs of people with the active respiratory disease. It is produced by mycobacteria, mainly *Mycobacterium tuberculosis*. In healthy people, infection often causes no symptoms, since the person's immune system acts to wall off the bacteria. Currently, a rising number of people contract TB (often accompanied by other bacterial infections) because their immune systems are compromised by immunosuppressive drugs, abuse substances, or HIV/AIDS, among others. Besides, the increasing emergence of multi-drug-resistant strains has also contributed to the alarming high morbidity and mortality of this endemia [2]. As a result, TB is one of the current leading causes of death in the world. The WHO estimates that about 30 million people will be infected in the next 20 years, not only in the developing countries but also in the developed world. Due to these facts TB currently receives a higher level of attention from health systems than other communicable diseases.

In view of the importance of this disease and the increasing incidence of drug-resistant strains, the investigation and development of new drugs is a leading area of research.

Two main approaches are currently being investigated for developing new anti-TB drugs [3]. One of them is based on the synthesis of analogues of existing drugs with the aim of shortening and improving TB treatment. The other one involves the search for novel structures that the mycobacteria have never been presented

☆ Part of this research was presented in the Brazilian patent of invention: M. Belén Tarallo, María H. Torre, D. Gambino, Clarice Q. Leite, Fernando R. Pavan, Patent PI0902923-0, 2009: Complexos de ferro-quinoxalina, processos de preparação dos mesmos e seus usos.

* Corresponding authors. Tel.: +598 2 9249739; fax: +598 2 9241906.
E-mail addresses: dgambino@fq.edu.uy (D. Gambino), mtorre@fq.edu.uy (M.H. Torre).

0162-0134/$ – see front matter © 2010 Elsevier Inc. All rights reserved.
doi:10.1016/j.jinorgbio.2010.07.005

with before. In the context of this second approach, our research is focused on the synthesis and characterization of new iron–quinoxaline derivative compounds with the aim of obtaining new and more potent anti-TB compounds which can improve the current chemotherapeutic treatments.

The study of quinoxaline derivatives has become of much interest in recent years because of their antibacterial, antiviral, anticancer, antifungal, antihelminthes and insecticidal activities [4]. Part of our group has been involved in the synthesis and biological assessment of a large amount of quinoxaline 1,4-di-*N*-oxide derivatives, including some of their metal complexes [5–10]. Some of these organic derivatives have shown excellent *M. tuberculosis* growth inhibition values. It has been observed that generally the lack of the two *N*-oxide groups has lead to the loss of the antimycobacterial activity [11–14]. On the other hand, the relationship between iron, mycobacteria and tuberculosis is well known. Treatment of several mycobacteria with *p*-aminosalicylic acid (PAS), one of the oldest antituberculosis drugs, resulted more effective when the cells were grown with adequate iron levels [15]. Besides, many iron complexes with different organic molecules showed antimycobacterial activity. For instance, $[Fe(CN)_5(isoniazide)]^{3-}$ appears to be a promising molecule for further drug development [16].

Taking into account these antecedents and due to the fact that during the last years we have been studying the effect of metal coordination on the bioactivity of selected 3-aminoquinoxaline-2-carbonitrile N^1,N^4-dioxide derivatives [5–10], we have recently developed two iron complexes, $[Fe^{III}(L–H)_3]$, with the derivatives **L1** and **L2** as ligands (Fig. 1) and have evaluated their antimycobacterial activity [17]. Having observed activity we decided to extend the work to other ligands of the same family. In this work we report the synthesis, characterization and *in vitro* evaluation of two further $[Fe^{III}(L–H)_3]$ complexes with L = **L3** and **L4** (Fig. 1). Both new complexes were characterized by elemental and conductimetric analyses and infrared (FTIR) and electronic spectroscopies. In addition, the compounds were studied by cyclic voltammetry and EPR spectroscopy. Mössbauer experiments were performed to get a deeper insight into the structure of the complexes. Their antimycobacterial activity was evaluated *in vitro* on *M. tuberculosis* $H_{37}Rv$ (ATCC 27294) and compared with that of the reference drug Isoniazid. In addition, cytotoxicity on eukaryotic cells was evaluated on cultured murine cell line J774.

2. Experimental

2.1. Materials

All common laboratory chemicals were purchased from commercial sources and used without further purification. The ligands **L1–L4** were synthesized by reaction of the corresponding benzofuroxan and malonitrile and characterized as previously described [18]. **L2** and **L4** were obtained as mixtures of 6- and 7-substituted isomers [18].

High purity dimethyl sulfoxide (DMSO) (Aldrich) was used for the electrochemical measurements. Tetrabutylammonium hexafluorophosphate $(TBA)PF_6$, from Fluka (electrochemical grade) was employed as supporting electrolyte. Extra-pure nitrogen was used to remove oxygen from the DMSO solutions.

2.2. Syntheses of the complexes $[Fe(L–H)_3]$

The complexes were synthesized by the following procedure: 0.12 mmol of L (25 mg **L1**, 28 mg **L2**, 32 mg **L3**, 32 mg **L4**) and 0.06 mmol (26 mg) of $Fe(NO_3)_3$ were mixed in methanol and reacted under reflux during 6 h. Purple solids were filtered off, washed with methanol and dried at room temperature.

$[Fe(\mathbf{L1}–H)_3]$; (code Fe–**L1**) yield: 74%. Anal. calc. for $C_{27}N_{12}H_{15}O_6Fe$: C, 49.19; H, 2.29; N, 25.49. Found: C, 49.21; H, 2.77; N, 25.59. Λ_M(DMSO): 1 μS/cm^2.

$[Fe(\mathbf{L2}–H)_3]\cdot 5H_2O$; (code Fe–**L2**) yield: 59%. Anal. calc. for $C_{30}N_{12}H_{31}O_{11}Fe$: C, 45.53; H, 3.00; N, 21.24. Found: C, 44.83; H, 2.57; N, 21.20. Λ_M(DMSO): 2 μS/cm^2. $[Fe(\mathbf{L3}–H)_3]\cdot H_2O$; (code Fe–***L3***) yield: 45%. Anal. calc. for $C_{30}N_{12}H_{20}O_{10}Cl_3Fe$: C, 41.33; H, 3.22; N, 16.18. Found: C, 41.35; H, 3.28; N, 16.28. Λ_M(DMSO): 8 μS/cm^2. $[Fe(\mathbf{L4}–H)_3]\cdot H_2O$; (code Fe–**L4**) yield: 80%. Anal. calc. for $C_{30}N_{12}H_{14}O_7F_9Fe$: C, 40.87; H, 1.60; N, 19.07. Found: C, 41.72; H, 1.39; N, 19.47. Λ_M(DMSO): 7 μS/cm^2.

Even though the C analysis results for Fe-L2 and Fe-L4 are not quite satisfactory, additional physicochemical characterizations of these compounds (see below) are consistent with their formulae.

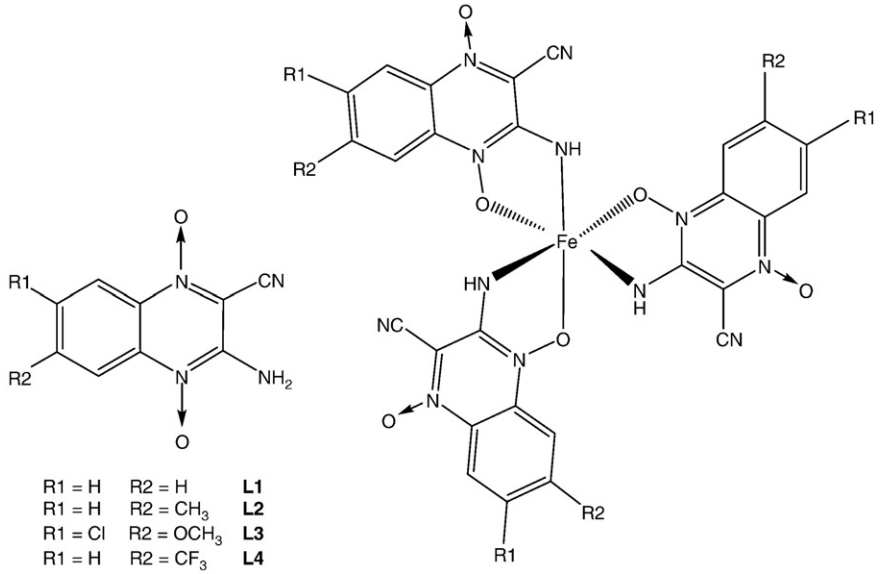

Fig. 1. Scheme showing the structure of the selected ligands (L) and the proposed structure for the iron(III) complexes $[Fe(L–H)_3]$. Selected ligands: L: **L1** = 3-aminoquinoxaline-2-carbonitrile N^1,N^4-dioxide, **L2** = 3-amino-6(7)-methylquinoxaline-2-carbonitrile N^1,N^4-dioxide, **L3** = 3-amino-6(7)-chloro-7(6)-methoxyquinoxaline-2-carbonitrile N^1,N^4-dioxide and **L4** = 3-amino-6(7)-trifluoromethylquinoxaline-2-carbonitrile N^1,N^4-dioxide.

2.3. Physicochemical characterization

C, H and N analyses were performed with a Carlo Erba Model EA1108 elemental analyzer. Conductimetric measurements were carried out at 25 °C in 10^{-3} M DMSO solutions using a Conductivity Meter 4310 Jenway [19]. Conductivity was measured during 24 h to assure the stability of the complexes in the solvent used for the microbiological studies. Electronic spectra of the complexes were registered on a Shimadzu UV-1603 spectrophotometer in DMSO solution. FTIR spectra (4000–400 cm^{-1}) of the complexes and the free ligands were measured as KBr pellets with a Bomen FTIR model MB102 instrument. Cyclic voltammograms were obtained with a PAR potentiostat/galvanostat model 263A controlled by the 270/250 Sofware (EG&G Princeton Applied Research). A printer and a standard electrochemical three electrode cell completed the system. Glassy carbon disc was employed as working electrode. A platinum wire was used as counter electrode, while an Ag/(10^{-3} M) $AgNO_3$ in CH_3CN/10^{-1} M (TBA)PF_6, was used as a reference electrode. This electrode was calibrated against the $[Fe(C_5H_5)_2]/[Fe(C_5H_5)_2]^+$ redox couple, for which a potential of +0.4 V *vs* normal hydrogen electrode (NHE) was assumed [20,21]. All potentials reported were referred to NHE in volts. Measurements were performed in oxygen purged 10^{-3} M DMSO solutions of the complexes containing 0.1 M (TBA)PF_6 as supporting electrolyte. A continuous gas stream was passed over the solution during the measurements. X-band (9.5 GHz) EPR spectra were measured on a Bruker ELEXSYS E580 system (Bruker BioSpin, Germany) at 10 K. The temperature was controlled with an Oxford ITC503 cryogenic system. Polycrystalline samples of the title compounds were drawn in a quartz EPR tube and then placed in the spectrometer rectangular cavity. All EPR data were corrected by subtracting a baseline corresponding to the EPR signal of the empty resonant cavity. Other acquisition conditions were: modulation amplitude, 1 mT; modulation frequency, 100 kHz; microwave power, 4 mW. The room temperature Mössbauer spectra were taken in transmission geometry using a conventional constant acceleration spectrometer of 512 channels with a 50 mCi nominal activity ^{57}Co source in a Rh matrix. The hyperfine parameters were obtained by fitting the data to lines of Lorentzian shape using a least-squares computer code with constraints. Isomer shifts are calibrated against an α-Fe foil at room temperature. According to the criterion of Long et al. [22], to obtain the optimum signal to noise ratio, the absorber thickness needed should be at least of 14 mg/cm^2 of Fe, which corresponds to an amount of compound of 137 mg/cm^2. Because the total amount of available compound was of only 104 mg, a special absorber holder was assembled which contained the whole available powder exposed to the gamma-ray beam in a cylinder of 8 mm diameter with a collimator that prevented any other ray to reach the detector.

2.4. Anti-M. tuberculosis activity assay

The anti-*M. tuberculosis* activity of the ligands and the iron complexes was determined by the Resazurin Microtiter Assay (REMA) [23]. Stock solutions of the test compounds were prepared in DMSO and diluted in Middlebrook 7H9 broth (Difco), supplemented with oleic acid, albumin, dextrose and catalase (OADC enrichment — BBL/Becton Dickinson, Sparks, MD, USA), to obtain final drug concentration ranges from 0.15 to 250 μg/mL. The serial dilutions were realized in Precision XS Microplate Sample Processor (Biotek™). The isoniazid was dissolved in distilled water, according to the manufacturers' recommendations (Difco laboratories, Detroit, MI, USA), and used as a standard drug. *M. tuberculosis* $H_{37}Rv$ ATCC 27294 was grown for 7 to 10 days in Middlebrook 7H9 broth supplemented with OADC, plus 0.05% Tween 80 to avoid clumps. Suspensions were prepared and their turbidities matched to the optical density of the McFarland no. 1 standard. After a further dilution of 1:25 in Middlebrook 7H9 broth supplemented with OADC, 100 μL of the culture were transferred to each well of a 96-well microtiter plate (NUNC), together with the test compounds. Each test was set up in triplicate. Microplates were incubated for 7 days at 37 °C, after which resazurin was added for the reading. Wells that turned from blue to pink, with the development of fluorescence, indicated growth of bacterial cells while maintenance of the blue color indicated bacterial inhibition [23,24]. The fluorescence was read (530 nm excitation filter and 590 nm emission filter) in a SPECTRAfluor Plus (Tecan) microfluorimeter. The MIC was defined as the lowest concentration resulting in 90% inhibition of growth of *M. tuberculosis* [23]. As a standard test, the MIC of isoniazid was determined on each microplate. The acceptable range of isoniazid MIC is from 0.015 to 0.05 μg/mL [23,24].

2.5. Citotoxicity assay

In vitro cytotoxicity assays (IC_{50}) were performed on the J774A.1 (ATCC TIB-67) cell line, as recommended by Ahmed et al. [25] and modified by us [26]. The cells were routinely maintained in Complete Medium (RPMI-1640 supplemented with 10% heat-inactivated fetal bovine serum (FBS); 100 U/mL penicillin and 100 μg/mL streptomycin), at 37 °C, in a humidified 5% CO_2 atmosphere. After reaching confluence, the cells were detached and counted. For the cytotoxicity assay, 1×10^5 cells/mL were seeded in 200 μL of Complete Medium in 96-well plates (NUNC). The plates were incubated at 37 °C under a 5% CO_2 atmosphere for 24 h, to allow cell adhesion prior to drug testing. The compounds were dissolved in DMSO and subjected to two-fold serial dilution from 1250 to 3.9 μg/mL. Cells were exposed to the compounds at various concentrations for a 24 h-period. Resazurin solution was then added to the cell cultures and incubated for 6 h. Cell respiration was followed as an indicator of cell viability and was detected by reduction of resazurin to resorufin, whose pink color and fluorescence indicates cell viability. A persistent blue color of resazurin is a sign of cell death [23,24]. The fluorescence measurements (530 nm excitation filter and 590 nm emission filter) were performed in a SPECTRAfluor Plus (Tecan) microfluorimeter. The IC_{50} value was defined as the highest drug concentration at which 50% of the cells are viable relative to the control [26]. A selectivity index (SI) was then calculated by dividing the IC_{50} by the MIC.

3. Results and discussion

Two new iron(III) [Fe(L–H)$_3$] complexes including the ligands **L3** (3-amino-6(7)-chloro-7(6)-methoxyquinoxaline-2-carbonitrile N^1, N^4-dioxide) and **L4** (3-amino-6(7)-trifluoromethylquinoxaline-2-carbonitrile N^1,N^4-dioxide) (Fig. 1) were synthesized with high purities and yields. Unfortunately, it was impossible to obtain single crystals adequate for a crystallographic study. Nevertheless, complexes could be adequately characterized in the same way as previously done for the reported copper, vanadium, palladium and iron compounds of this family of ligands by using a combination of several physicochemical methods [5–10]. Both complexes are neutral non conducting compounds in DMSO. Analytical and conductimetric results are in agreement with the proposed formula and structure (Fig. 1). The conductivity was measured during 24 h and no major changes were observed, demonstrating the stability of the complexes in DMSO solution. Similar results were obtained by means of the electrochemical measurements. The visible spectra of the ligands showed two strong bands in the 508–510 nm and 363–368 nm ranges. These bands obscured the predicted spin allowed d–d transitions for the iron species. Therefore structural information could not be obtained from these spectra.

3.1. Cyclic voltammetry

Cyclic voltammograms (CV) were run at incremental scan rates (v) from 0.05 V/s to 2.0 V/s. Results for compounds **L3** and Fe–**L3** were not

included in the electrochemical study because they exhibited an erratic voltammetric pattern; CV changes with time and no reproducible curves were obtained. To exemplify the general electrochemical behavior of the complexes the reduction of Fe–**L1** and Fe–**L2** complexes was studied at different scan rates (ν) using glassy carbon as working electrode in DMSO solutions and was compared with those obtained for the free ligands.

L1 and **L2** showed a similar behavior to that previously obtained in this laboratory and discussed in detail with analogous compounds using Pt as working electrode [10].

Comparison of the data reveals that no appreciable effects can be ascribed to the electrode material. The voltammogram obtained for **L1** at v = 0.1 V/s, is shown in Fig. 2. Reduction peak potential values at v = 0.1 V/s are summarized in Table 1.

The ligands exhibit two reduction processes (labeled A and B) at very close potentials, during the forward negative scan. As discussed in detail elsewhere [10], the first electron addition corresponds to the reduction of the N^1,N^4 dioxide derivatives to a radical anion with addition of a proton to the N–O group (see Scheme 1). After this step cleavage of the N–OH bond occurs to give the mono-*N*-oxide compound and the hydroxyl radical. The second electron addition is consistent with the reduction and subsequent loss of the second oxide group. These processes are followed by the quasi-reversible reduction of the heterocycle itself (couple C/C′). The oxidation of a new electroactive compound generated during the reduction cycle occurs at potentials of peak D.

The cyclic voltammetric behavior of the complexes is similar to that illustrated for the free ligands, but some differences are observed. The complexes show a new peak (I) which corresponds to the reduction of the metallic center from Fe(III) to Fe(II), on the forward cathodic scan (Fig. 3 and Table 1). The species generated on this path is stable on the time scale of the experiment, hence, giving rise to the return peak (I′) in the voltammogram. The redox process (I/I′) is quasi-reversible (ΔEp>60 mV) and the ratio of anodic to cathodic peak currents (i_{pa}/i_{pc}) is near unity at all scan rates investigated (see Fig. 3b) [27]. The current peak (I) of process increases with the square root of the scan rate ($\nu^{1/2}$), approaching a single straight-line plot, in accordance with diffusion control (see inset in Fig. 3b). Moreover, as can be seen in Fig. 3a and b, the current peak of the second reduction (AB) is approximately twice of the first one. From this fact and from reduction potential data we can infer that reduction processes labeled A and B in the free ligands appear closely overlapped in the voltamperometric response of the complexes (peak AB). Furthermore, as ν increases the anodic counterpart of this peak is observed during the reverse anodic scan in contraposition with the response of the free ligand. The process appears to become more reversible when the voltage scan is reversed before process C takes place and with increasing scan rate (see inset of Fig. 3b). Thus, the coordination modifies the electrochemical behavior of the species formed during these reduction paths.

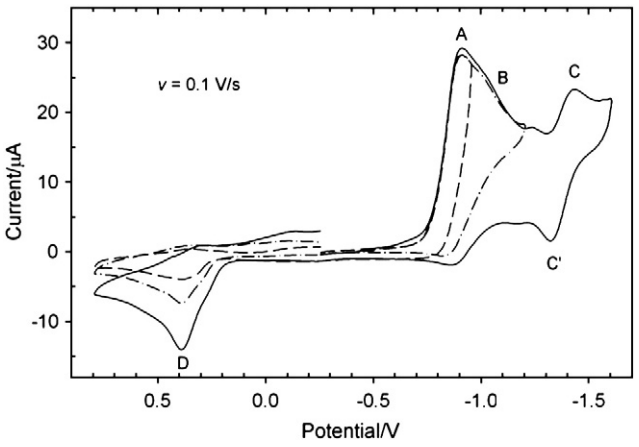

Fig. 2. Cyclic voltammograms at different potential limits of 1 mM **L1** in DMSO solution. Scan rate v = 0.1 V/s.

Table 1
Electrode potentials (in V *vs* NHE) of selected complexes and the free ligands at ν = 0.1 V/s.

Compound	Epc(I)/Epa(I′)	Epc(A)	Ep(B)	Epc(AB)	Epc(C)
L1	–	−0.92	−1.04	–	−1.44
Fe–L1	−0.61/−0.53	–	–	−0.96	−1.42
L2	–	−0.82	−0.97	–	−1.48
Fe–L2	−0.62/−0.53	–	–	−0.98	−1.39

In summary, results show that the reduction potential of both iron compounds are similar and fall in the range previously reported for other metal complexes of the same family of ligands. Despite this fact and although a higher number of compounds would be needed for establishing general conclusions, their behavioral analogy would suggest that no apparent correlation exists between their redox chemistry and their biological activity.

3.2. Spectroscopic measurements

3.2.1. IR spectra

The IR spectra of both new complexes were compared with those of the free ligands and the previously reported Cu, V, Pd and Fe complexes [5–10,17]. So, taking into account our previous knowledge on vibrational behavior of 3-aminoquinoxaline-2-carbonitrile N^1,N^4-dioxide derivatives metal complexes, vibration bands related with the ligand's coordination mode were tentatively assigned. Selected vibration bands and their assignments are depicted in Table 2.

All the complexes showed a similar spectroscopic behavior. Both strong bands corresponding to $\nu_{as}(NH_2)$ and $\nu_s(NH_2)$ of the amino group, located for the free ligands in the 3400 and 3250 cm^{-1} region, disappeared after coordination and only one band (ν(NH)) of medium intensity around 3300 cm^{-1} was observed. This is in accordance with the presence of a secondary amine formed by deprotonation of the primary amine as a consequence of the coordination with iron ion. This behavior was previously observed for vanadyl, palladium and copper complexes with this family of ligands, and for metal chelates with aromatic ligands involving the amino group in ortho position to the *N*-oxide [5–10,17,28]. Besides, the strong ν(N→O) band for the free ligands turned weak upon complexation indicating the coordination of one N→O group per ligand molecule keeping the other uncoordinated as shown in Fig. 1. In the case of Fe–**L2** the disappearance of the strong ν(N→O) band in the characteristic range was probably due to the fact that the uncoordinated N→O groups have additional interactions with other atoms from neighboring molecules, which form intermolecular bonds in the solid state. This behavior was previously observed in related copper complexes [9]. In addition changes in the ν(CN→O) bands were observed due to complexation. The ν(C≡N) (2221–2246 cm^{-1}) suffered only minor changes upon complexation in agreement with the fact that this group did not coordinate to iron ion. Taking into account the stoichiometry found and the infrared spectral data, the proposed structures for the complexes are shown in Fig. 1.

3.2.2. EPR spectra

The set of resonances observed in the experimental EPR spectra (Fig. 4) can be interpreted on the basis of the spin Hamiltonian: H = βg$_0$.B.S + S.D.S, where β is the Bohr magneton, B is the applied magnetic field, and D is the zero-field tensor used for S>1/2 systems. The zero-field term accounts for the deviations of the g-values from 2.0, thus giving rise to an effective g-value (g_{eff}), and its components

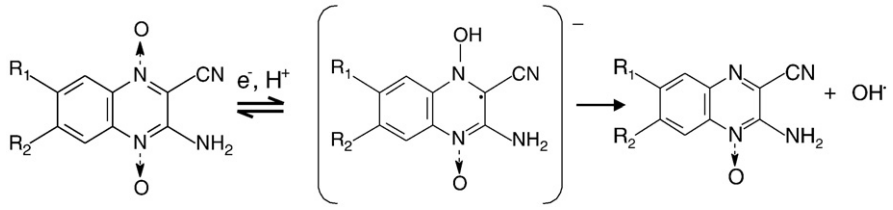

Scheme 1. Reduction steps of the N^1,N^4 dioxide derivatives.

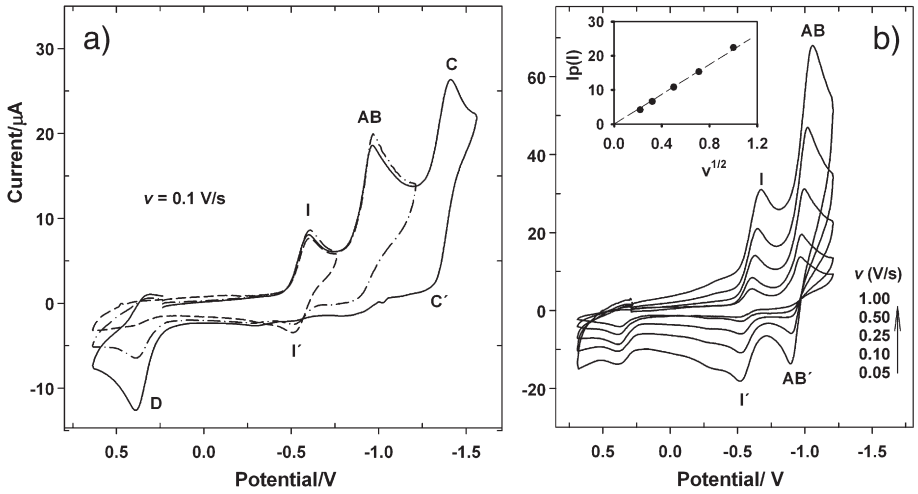

Fig. 3. Cyclic voltammograms of 1 mM Fe–**L1** in DMSO solution: a) at different cathodic limits, v = 0.1 V/s; b) between +0.70 V and −1.20 V, at different scan rates. Inset of the b: dependence of the cathodic current peak (I) on the square root of the scan rate.

(D and E) give information on the ligand coordination [29]. The low temperature EPR spectra from polycrystalline samples of the Fe compounds under study (Fe–**L1**, Fe–**L2**, Fe–**L3**, and Fe–**L4**) are all characterized by a main intense resonance centered around 160 mT that, when converted to g-value, gives an effective g of *ca.* 4.3. For Fe–**L1**, Fe–**L2**, and Fe–**L4**, a weak resonance around 80 mT (g_{eff}~9) was observed. These EPR signals are characteristic of magnetically isolated high-spin Fe(III) in a rhombic environment [30,31] and arise from transitions between $m_S = \pm 1/2$ (g_{eff}~9) or $m_S = 3/2$ (g_{eff}~4.3) states. The somewhat broader linewidth of the g_{eff}~4.3 resonance can be taken as a measure of the structural heterogeneity of the Fe centers within the sample. The appearance of broad lines, especially in the spectra of Fe–**L1** and Fe–**L3**, is probably due to deviations of the local symmetry around the Fe(III) ions from a fully rhombic (characterized by a ratio E/D = 1/3).

Table 2
Tentative assignment of selected IR bands of the new iron complexes. Bands for the free ligands and the previously reported Fe(III) complexes are included for comparison.

Compound	ν_{as}(N–H)	ν_s(N–H)	ν_s(N–H)	ν(CN)	ν(N→O)
L1	3353 (s)	3262 (s)		2237 (w)	1343 (s)
Fe–L1	–	–	3299 (s)	2221 (w)	1340 (vw)
L2	3331 (s)	3260 (m)		2232 (w)	1333 (s)
Fe–L2	–	–	3314 (m)	2222 (w)	–
L3	3365 (s)	3282 (m)		2238 (w)	1341 (s)
Fe–L3	–	–	3327 (s)	2233 (w)	1340 (vw)
L4	3401 (s)	3282 (m)		2246 (w)	1348 (*vs*)
Fe–L4	–	–	3366 (s)	2237 (w)	1343 (vw)

ν: stretching; ν_{as}: asymmetric stretching, ν_s: symmetric stretching, s: strong, m: medium, w: weak, vw: very weak. Band positions are given in cm^{-1}.

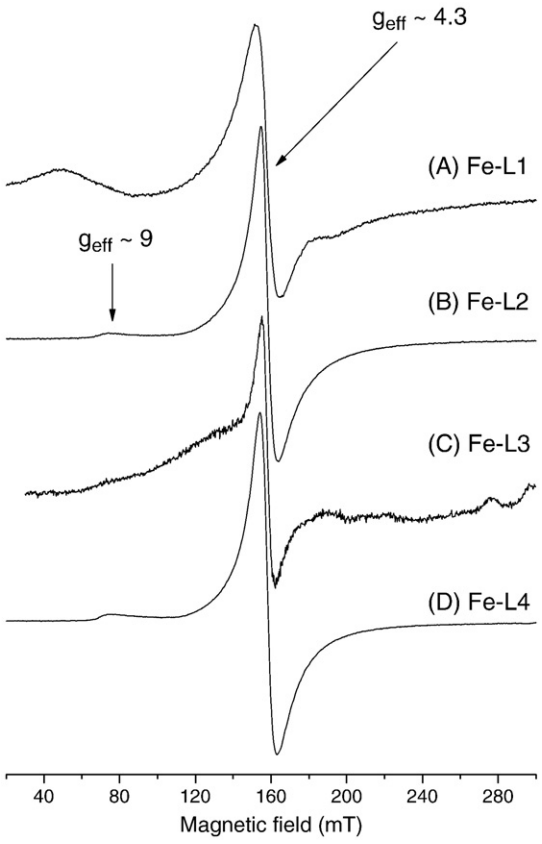

Fig. 4. EPR spectra from polycrystalline samples of the Fe compounds measured at 10 K.

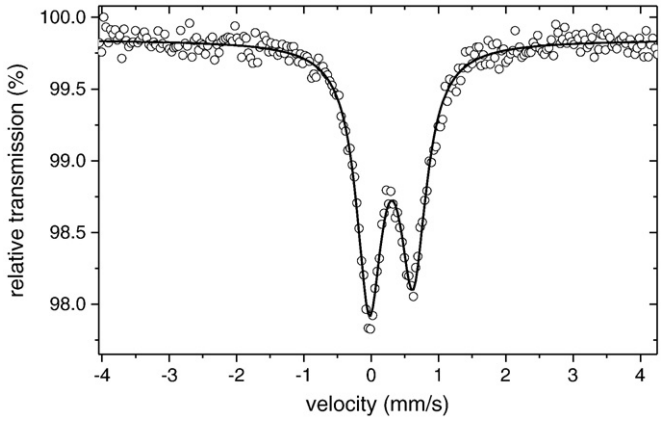

Fig. 5. Room temperature Mössbauer spectrum of [Fe(**L1**–H)$_3$]. The hollow circles are the experimental points and the solid line is the result of the least-squares fitting described in the text using the parameters shown in Table 3.

3.2.3. Mössbauer spectra

The room temperature Mössbauer spectrum displays only one central doublet (Fig. 5). The hyperfine parameters, shown in Table 3, are typical of high-spin Fe(III) ions in a not too distorted environment. There is a difference in the line intensities of the doublet. This difference may be due to the trend of the sample to texture in the absorber holder, *i.e.*, the powder orients itself in a preferred orientation with respect to the crystalline axes which made the L_1/L_2 ratio to be different from the 1:1 expected ratio for a randomly oriented polycrystalline sample. It might be due also to the well known asymmetry which is a common feature of high-spin Fe(III) compounds like $FeCl_3 \cdot 6H_2O$ [32,33].

3.3. Anti-M. tuberculosis activity

Both new complexes were evaluated *in vitro* for their antimycobaterial activities on *M. tuberculosis* $H_{37}Rv$ (ATCC 27294). Results were compared to those of both previously reported iron(III) complexes and the reference drug Isoniazid. The minimum inhibitory concentration (MIC) values are depicted in Table 4.

All the ligands and the complexes were active against *M. tuberculosis*. Iron complexes of **L2**, **L3** and **L4** resulted more active than the corresponding free ligands, demonstrating that metal coordination can favorably modify the profile of antimycobacterial activity of 3-aminoquinoxaline-2-carbonitrile N^1,N^4-dioxide derivatives. Only the previously reported **L1** complex showed less activity than the free ligand. Both newly developed iron complexes showed significantly higher activity than the other complexes and the free ligands. As previously reported for related copper, vanadyl and palladium complexes [5–10], the change of the substituents on the quinoxaline moiety produced significant differences in biological activity. The MIC values of **L3** and **L4** iron complexes (0.78 μg/mL) are comparable or better than those of some "second-line" drugs in clinical use as streptomycin (MIC = 1.00 μg/mL), ciprofloxacin (MIC = 6 μM, 2.00 μg/mL), *p*-aminosalicylic acid (MIC = 3.3–13.1 μM, 0.5–2.0 μg/mL), ethionamide (MIC = 3.8–7.5 μM, 0.63–1.25 μg/mL), cycloserine (MIC = 122–490 μM, 12.5–50 μg/mL), gentamicin (MIC = 2.0–4.0 μg/mL), ethambutol (MIC = 4.6–9.2 μM, 0.94–1.88 μg/mL), kanamycin (MIC = 1.25–5.0 μg/mL), tobramycin (MIC = 2.8–5.6 μM, 4.0–8.0 μg/mL), clarithromycin (MIC = 10.7–21.4, 8.0–16 μg/mL) and thiacetazone (MIC = 0.53–8.5 μM, 0.125–2.0 μg/mL) [24,34,35].

Iron is an essential nutrient for all living organisms. It is well known that microorganisms and particularly *M. tuberculosis* have evolved specialized iron transport systems to include iron inside the cells. The developed iron complexes could act as carriers of the bioactive ligands, producing a concentration increase of these molecules inside the mycobacteria cells.

Table 3
Hyperfine parameters yielded by the least square fitting to lorentzian lines of the spectrum.

Δ (mm/s)	δ (mm/s)[a]	L_1/L_2	Γ (mm/s)
0.65 ± 0.03	0.40 ± 0.01	1.14 ± 0.02	0.46 ± 0.01

[a] The isomer shift δ is referred to a foil of α-Fe at room temperature.

Table 4
MIC values (μg/mL, μg of L/mL and μM) of the Fe(III) complexes and the free ligands against *M. tuberculosis* $H_{37}Rv$ (ATCC 27294).

Compound	MIC (μg/mL)[a]	MIC (μg of L/mL)[b]	MIC (μM)[c]	IC_{50} (μg/mL)[d]	SI[e]
Fe–L1	7.8	7.1	11.8	156.3	20
Fe–L2	3.9	3.2	4.9	156.3	40
Fe–L3	0.78	0.67	0.89	312.5	400
Fe–L4	0.78	0.69	0.87	19.5	25
L1	5.0	5.0	24.7	156.3	31
L2	6.2	6.2	28.7	156.3	25
L3	3.9	3.9	14.5	312.5	80
L4	6.2	6.2	22.7	39.0	6

[a] MIC: minimum inhibitory concentration in μg/mL.
[b] MIC: minimum inhibitory concentration recalculated considering μg of ligand L included per μg of complex Fe–L.
[c] MIC: minimum inhibitory concentration in μM.
[d] IC_{50}: 50% inhibitory concentration on J774 murine cells.
[e] SI: selectivity index = IC_{50}/MIC(μg/mL).

3.4. Unspecific cytotoxicity on murine J774 cells

Table 4 shows the IC_{50} values of the complexes and the ligands on mammalian cells. All of them presented low citotoxicity, with high selectivity indexes SI (selectivity index = IC_{50}/MIC). Usually, compounds showing SI values higher than 10 are considered suitable to be further evaluated as potential anti-TB drugs. All the iron complexes showed SI values higher than 20. SI values depicted in Table 4 show that particularly Fe**–L3** has a very low MIC value (high inhibitory activity) and a very low cytotoxicity. It constitutes a promising new potent chemotherapeutic alternative to be further evaluated *in vivo* in experimental models of TB.

4. Conclusions

Two new Fe(III) complexes with selected 3-aminoquinoxaline-2-carbonitrile N^1,N^4-dioxide derivatives as ligands, [Fe(L–H)$_3$], have been synthesized in satisfactory yields and characterized by different techniques. The novel complexes showed *in vitro* bacteriostatic or bactericide activity on the causative agent of TB *M. tuberculosis*, showing very low unspecific cytotoxicities on eukaryotic cells. Both showed higher inhibitory effects than the "second-line" therapeutic drugs. Accordingly, these compounds could be useful as hospital desinfectants, as therapeutical agents for instance for the treatment of skin infections produced by mycobacteria together with antiseptics and/or as drugs for the treatment of TB or other mycobacterioses. Further work is in progress in order to get more biological details of the action of these compounds on *M. tuberculosis* and to further evaluate these promising compounds.

Acknowledgments

The authors are grateful to CYTED (thematic network RIIDFCM 209RT0380) and PEDECIBA Química (Uruguayan Programme for the Development of Basic Sciences, Chemistry Area) for financial support.

References

[1] http://www.who.int/.
[2] P.G. Smith, A.R. Moss, Epidemiology of tuberculosis, in: B.R. Bloom (Ed.), Tuberculosis, Pathogenesis, Protection and Control, ASM Press, Washington, 1994, pp. 47–61.
[3] D. Sriram, P. Yogeeswari, R. Devakaram, Bioorg. Med. Chem. 14 (2006) 3113–3118.
[4] S.A. Khan, K. Saleem, Z. Khan, Eur. J. Med. Chem. 42 (2007) 103–108.
[5] C. Urquiola, M. Vieites, M.H. Torre, M. Cabrera, M.L. Lavaggi, H. Cerecetto, M. González, A. López de Cerain, A. Monge, P. Smircich, B. Garat, D. Gambino, Bioorg. Med. Chem. 17 (2009) 1623–1629.
[6] C. Urquiola, D. Gambino, M. Cabrera, M.L. Lavaggi, H. Cerecetto, M. González, A. López de Cerain, A. Monge, A.J. Costa-Filho, M.H. Torre, J. Inorg. Biochem. 102 (2008) 119–126.
[7] C. Urquiola, M. Vieites, G. Aguirre, A. Marín, B. Solano, G. Arrambide, M.L. Lavaggi, M.H. Torre, M. González, A. Monge, D. Gambino, H. Cerecetto, Bioorg. Med. Chem. 14 (2006) 5503–5509.
[8] P. Noblía, M. Vieites, M.H. Torre, A.J. Da Costa Filho, H. Cerecetto, M. González, M.L. Lavaggi, Y. Adachi, H. Sakurai, D. Gambino, J. Inorg. Biochem. 100 (2006) 281–287.
[9] M.H. Torre, D. Gambino, J. Araujo, H. Cerecetto, M. González, M.L. Lavaggi, A. Azqueta, A. López de Cerain, A. Monge-Vega, U. Abram, A.J. Costa-Filho, Eur. J. Med. Chem. 40 (2005) 473–483.
[10] M. Vieites, P. Noblía, M.H. Torre, H. Cerecetto, M. Lavaggi, A. Costa Filho, A. Azqueta, A. López de Cerain, A. Monge, B. Parajón-Costa, M. González, D. Gambino, J. Inorg. Biochem. 100 (2006) 1358–1367.
[11] Y. Sainz, M.E. Montoya, F.J. Martínez-Crespo, M.A. Ortega, A. López de Ceráin, A. Monge, Arzneim.-Forsch. Drug Research 1 (1999) 55–61.
[12] M.E. Montoya, Y. Sainz, M.A. Ortega, A. López de Ceráin, A. Monge, Il Farmaco 53 (1998) 570–573.
[13] B. Zarranz, A. Jaso, I. Aldana, A. Monge, Bioorg. Med. Chem. 11 (2003) 2149–2156.
[14] A. Jaso, B. Zarranz, I. Aldana, A. Monge, Eur. J. Med. Chem. 38 (2003) 791–800.
[15] C. Ratledge, Tuberculosis 84 (2004) 110–130.
[16] J.S. Oliveira, E.H.S. Souza, L.A. Basso, M. Palaci, R. Dietze, D.S. Santos, I.S. Moreira, Chem. Comm. (2004) 312–313.
[17] M.B. Tarallo, C. Urquiola, A. Monge, F.R. Pavan, C.Q. Leite, M.H. Torre, D. Gambino, Met. Ions Biol. Med. 10 (2008) 865–872.
[18] A. Monge, F.J. Martínez-Crespo, A. López de Ceráin, J.A. Palop, S. Narro, V. Senador, A. Marín, Y. Sáinz, M. González, E. Hamilton, A.J. Barker, J. Med. Chem. 38 (1995) 4488–4494.
[19] W.J. Geary, Coord. Chem. Rev. 7 (1971) 81–91.
[20] H.M. Koepp, H. Went, H.Z. Strehlow, Z. Elektrochem. 64 (1960) 483–491.
[21] R.R. Gagné, C.A. Koval, G.C. Lisensky, Inorg. Chem. 19 (1980) 2854–2855.
[22] G.J. Long, T.E. Cranshaw, G. Longworth, Mössbauer Effect Reference and Data Journal 6 (1983) 42–49.
[23] J.C. Palomino, A. Martin, M. Camacho, H. Guerra, J. Swings, F. Portaela, Antimicrob. Agents Chemother. 46 (2002) 2720–2722.
[24] L.A. Collins, S.G. Franzblau, Antimicrob. Agents Chemother. 41 (1997) 1004–1009.
[25] S.A. Ahmed, R.M. Gogal, J.E. Walsh, J. Immunol. Methods 170 (1994) 211–224.
[26] F.R. Pavan, P.I.S. Maia, S.R.A. Leite, V.M. Deflon, A.A. Batista, D.N. Sato, S.G. Franzblau, C.Q.F. Leite, Eur. J. Med. Chem. 45 (2010) 1898–1905.
[27] J. Bard, L.R. Faulkner, Electrochemical Methods, 2nd.EditionJ. Wiley, New York, 2001.
[28] N.M. Karayannis, L.L. Pytlewski, C.M. Mikulski, Coord. Chem. Rev. 11 (1973) 93–159.
[29] T. Castner, G.S. Newell, W.C. Holton, C.P. Slichter, J. Chem. Phys. 32 (1960) 668–673.
[30] H.H. Wickman, M.P. Klein, D.A. Shirley, J. Chem. Phys. 43 (1965) 2113–2117.
[31] R.D. Dowsing, J.F. Gibson, J. Chem. Phys. 50 (1969) 294–303.
[32] N. Thrane, G. Trumpy, Phys. Rev. B 1 (1970) 153–155.
[33] A. Majumder, G. Pilet, M. Salah El Fallah, J. Ribas, S. Mitra, Inorg. Chim. Acta 360 (2007) 2307–2312.
[34] D. Sriram, P. Yogeeswari, R. Thirumurugan, Bioorg. Med. Chem. Lett. 14 (2004) 3923–3924.
[35] R.P. Tripathi, N. Tewari, V.K. Dwivedi, Med. Res. Rev. 25 (2005) 93–131.